

# The Design and Generation of Inorganic Cylindrical Cage Architectures by Metal-Ion-Directed Multicomponent Self-Assembly

Paul N. W. Baxter,<sup>[a]</sup> Jean-Marie Lehn,<sup>\*[a]</sup> Gerhard Baum,<sup>[b]</sup> and Dieter Fenske<sup>[b]</sup>

**Abstract:** The inorganic cage-type architectures **1–6** and **10** of cylindrical shape and nanometric size are generated spontaneously by self-assembly from the linear ditopic ligands **7a–f** and **9**, the circular tritopic ligand **8** and copper(I) or silver(I) ions. The crystal structures of two such complexes have been determined. They confirm and provide a detailed description of the geometry of these species. They also indicate that the

anions are contained within the central cavity. An experiment performed with a mixture of the ligands **7a**, **7c**, and **7d** shows that self-assembly occurs with ligand selection, only the expected com-

**Keywords:** inorganic architectures • metal complexes • nanostructures • self-assembly • supramolecular chemistry

plexes **1a**, **3**, and **4** being formed. The self-assembly is also influenced by the nature of the counteranions. The results demonstrate that supramolecular architectures of well-defined shape and nanometric size are accessible by multicomponent self-assembly processes involving several ligands of different types and several metal ions. They open ways towards the spontaneous but directed generation of complex nanostructures.

## Introduction

Closed three-dimensional molecular cage-type structures that have the capability of acting as receptor molecules that encapsulate guest species have provided the chemical community with a continual source of fascination and study over the past three decades. A variety of such molecules encompassing several classes of compounds have been prepared. For example, cryptates were developed for alkali metal ion and anion binding,<sup>[1]</sup> multiwalled cyclophanes<sup>[2]</sup> and carceplexes<sup>[3a,b]</sup> encapsulate neutral molecular guests, and inorganic clusters enclose various cations and anions.<sup>[4]</sup> Such compounds may present a range of applications in materials science, medicine, and chemical technology. Additionally, the unusual properties of these systems provide interesting and challenging opportunities for the study of basic physicochemical issues. However, access to these substances through the methodologies of molecular chemistry makes them of limited availability, thus posing also a serious obstacle to their technological development, due to the lengthy multistep

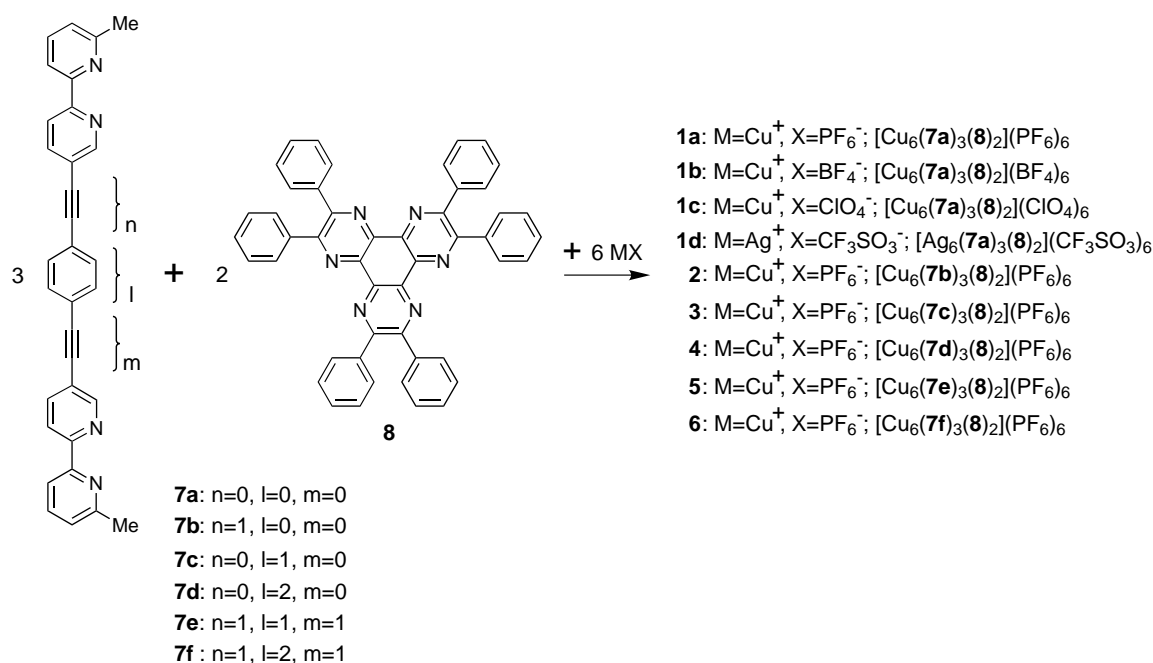
reaction sequences and low overall yields often encountered during their synthesis.<sup>[1]</sup>

A conceptually different approach of high promise lies within supramolecular chemistry and is provided by the processes of self-assembly and self-organization.<sup>[5]</sup> Recently molecular cages have been prepared in high to quantitative yield through self-assembly from simpler components, through hydrogen bonding<sup>[6a–c]</sup> and metal-ion–ligand interactions.<sup>[7, 8a–p]</sup> As well as currently providing one of the potentially most efficient methods of access to cage-type molecules, this approach offers insight into the process of formation of large biomolecular assemblies such as virus and bacterial capsids.<sup>[9]</sup> The work presented herein describes the use of multicomponent metal-ion–ligand self-assembly as a building principle for the controlled generation of molecular cage complexes of up to nanodimensional size and predetermined shape.

**Design concept:** Early investigations showed that it was possible to use metal-ion–ligand interactions as a driving force for the generation of structural complexity at a molecular level. This approach allowed direct access to topographically unusual metal ion containing entities such as helicates,<sup>[10, 11]</sup> catenates,<sup>[12]</sup> and metallomacrocyclic receptors.<sup>[13]</sup> The general design principle may also allow the self-assembly of three-dimensional architectures such as molecular cages and cage-type receptors of controllable size and shape, from multiple ligand components and metal ions. Inorganic cage architectures that incorporate metal ions as

[a] Prof. Dr. J.-M. Lehn, Dr. P. N. W. Baxter  
Laboratoire de Chimie Supramoléculaire, ISIS-ULP  
4, rue Blaise Pascal, F-67000 Strasbourg (France)  
Fax: (+33) 388 41 10 20  
E-mail: lehn@chimie.u-strasbourg.fr

[b] G. Baum, Prof. Dr. D. Fenske  
Institut für Anorganische Chemie, Universität Karlsruhe  
Engesserstrasse, Geb.-Nr. 30.45, D-76128 Karlsruhe (Germany)



Scheme 1. Multicomponent self-assembly of the cylindrical architectures **1–6** from the linear ditopic **7** and circular tritopic **8** ligands, and copper(i) or silver(i) cations.

integral structure-generating units would be expected to exhibit novel and interesting physicochemical properties such as optical, magnetic, electrochemical, and catalytic functions.

As a first step we envisioned the self-assembly of the  $C_3$  symmetric cage complex **1** (Scheme 1, Figure 1).<sup>[7]</sup> The concept for its design was based on the following reasoning: i) it is constructed from bipyridine subunits and metal ions of tetrahedral coordination geometry, a combination which had already been demonstrated to participate in self-assembly reactions;<sup>[10–12]</sup> ii) structure **1** is the only entity in the reaction mixture in which all the ligand-binding sites are occupied by metal ions and all metal ions are fully coordinated by ligands;

complex **1** therefore represents the situation of maximum site occupancy and must be the most stable species produced in the reaction; iii) the ligand components of **1** are rigidly preorganized; this feature would be expected to reduce entropic penalties associated with loss in degrees of rotational freedom upon self-assembly; iv) ligand **8** in cage **1** bears groups of sufficient steric requirements to destabilize polymer formation in the presence of metal ions; this would be expected to generate a reservoir of energetically less stable monomers and oligomers comprising **8** and metal ions with incompletely occupied sites; initial investigations showed that phenyl rings would be sufficient for this purpose;<sup>[14]</sup> v) the presence of phenyl substituents on **8** was also expected to stabilize the cage **1** superstructure by maximizing intramolecular aromatic  $\pi$ - $\pi$  interactions between the electron-deficient pyridine rings of **7a** and the phenyl rings of **8**.

**Abstract in French:** *Les architectures inorganiques 1-6 et 10 de forme cylindrique et de taille nanométrique se forment spontanément par auto-assemblage à partir des ligands ditopiques linéaires 7 et 9, du ligand tritopique circulaire 8 et de cations cuivre(i) ou argent(i). Les structures cristallines de deux de ces complexes ont été déterminées. Elles confirment la géométrie de ces espèces et en permettent une description détaillée. Elles indiquent aussi que des anions sont contenus dans leur cavité centrale. Une expérience menée avec un mélange des ligands 7a, 7c et 7d conduit à la formation exclusive des complexes attendus 1a, 3 et 4, indiquant que l'auto-assemblage se fait avec sélection des ligands. Il est aussi influencé par la nature des contre-ions. Ces résultats démontrent que des architectures supramoléculaires de forme bien définie et de taille nanométrique sont rendues accessibles par des processus d'auto-assemblage à composants multiples mettant en jeu plusieurs ligands de différents types et plusieurs ions métalliques. Ils ouvrent la voie à la formation spontanée mais contrôlée de nanostructures complexes.*

## Results and Discussion

**Self-assembly of the cylindrical complexes 1a–1d:** When nitromethane was added to a 1.5:1:3 stoichiometric ratio of **7a**,<sup>[7]</sup> **8**,<sup>[15]</sup> and  $[Cu(MeCN)_4]PF_6$  and the reaction mixture stirred at ambient temperature, the ligand components reacted to give the deep purple cage complex **1a** in quantitative yield. <sup>1</sup>H NMR measurements of the solution 24 h after mixing showed a simple spectrum comprising ten bands, two triplets, and a doublet due to **8** and seven bands from **7a**, corresponding to the presence of a single highly symmetric species in solution. A similar spectrum is obtained for the corresponding tetrafluoroborate compound **1b** (Figure 2). The <sup>13</sup>C spectrum also showed the expected seventeen bands. Addition of a small quantity of **7a** or **8** to a nitromethane solution of the product complex resulted in compli-

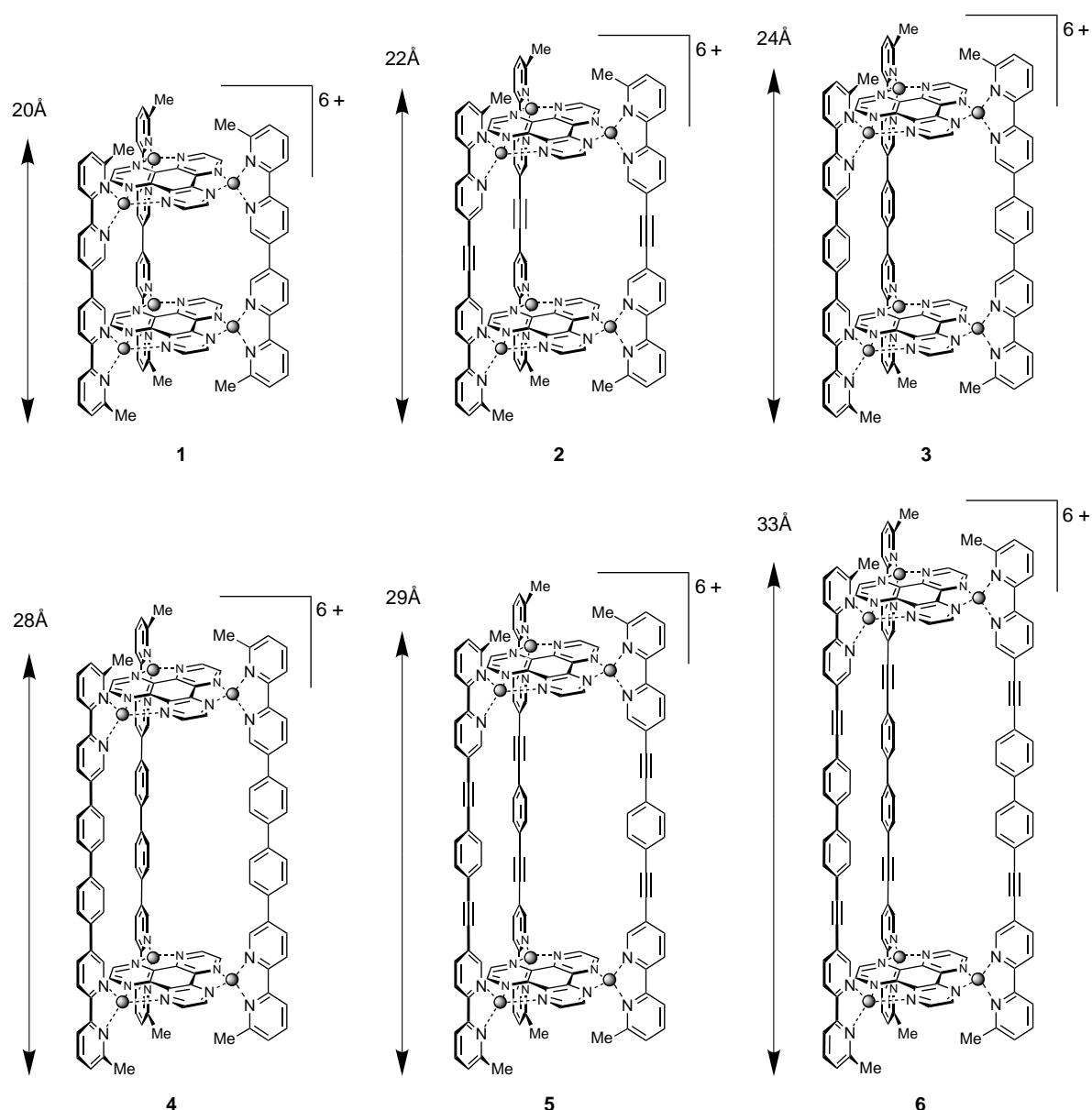


Figure 1. Schematic representations of the structures of the cylindrical inorganic cage architectures **1–6** of nanometric size; the heights of the complexes are indicated with inclusion of the Van der Waals surfaces (phenyl rings on **8** omitted for clarity).

cation of the  $^1\text{H}$  NMR spectrum with sharp peaks due to **1a** still present as a major component. Thus **1a** is undergoing slow exchange on the NMR timescale in nitromethane solution. The visible spectrum of a 1:1 mixture of  $[\text{Cu}(\text{MeCN})_4]\text{PF}_6$  and **8** in  $\text{CH}_2\text{Cl}_2$  gave absorptions at 509 and 613 nm, and that of a 1:1 mixture of  $[\text{Cu}(\text{MeCN})_4]\text{PF}_6$  and **7a** in 5%  $\text{MeCN}/\text{CH}_2\text{Cl}_2$  at 472 nm. However, absorptions due to the homoligand chromophoric units  $[\text{Cu}(\mathbf{7a})_2]^+$ , and  $[\text{Cu}(\mathbf{8})_2]^+$  were absent in the visible spectrum of the reaction product which instead showed two absorptions at 546 and 695 nm in  $\text{CH}_2\text{Cl}_2$ . This showed that entities incorporating the mixed ligand chromophore  $[\text{Cu}(\mathbf{7a})(\mathbf{8})]^+$  were the dominant species present in solutions of the above reaction product, further supporting its formulation as the cage complex **1a**. The electrospray (ES) mass spectrum recorded at  $10^{-4}$   $\text{mol dm}^{-3}$  in nitromethane showed four bands corresponding to

the species  $[\text{Cu}_6(\mathbf{7a})_3(\mathbf{8})_2](\text{PF}_6)_4]^{2+}$ ,  $[\text{Cu}_6(\mathbf{7a})_3(\mathbf{8})_2](\text{PF}_6)_3]^{3+}$ ,  $[\text{Cu}_6(\mathbf{7a})_3(\mathbf{8})_2](\text{PF}_6)_2]^{4+}$ , and  $[\text{Cu}_6(\mathbf{7a})_3(\mathbf{8})_2](\text{PF}_6)]^{5+}$ , formed by successive counterion loss. Cation **1** was also found to self-assemble in quantitative yield in the presence of other anions, for example  $\text{BF}_4^-$  (**1b**) and  $\text{ClO}_4^-$  (**1c**).

Complex **1b** was characterized by X-ray crystallography, thereby providing unambiguous evidence for the cage-type structure of **1**.<sup>[7]</sup> The cation consists of a triple helical arrangement of three **7a** ligands forming the walls of the cage, capped top and bottom by two horizontally positioned **8** ligands and held together by six  $\text{Cu}^+$  ions. The overall dimensions of **1b** are 19.0 (height)  $\times$  20.0 (diameter) Å placing it within the nanostructural domain. The cage also possesses an internal void of approximately  $4 \times 6$  Å (taking Van der Waals radii into consideration) in which some residual electron density was located but not identified.

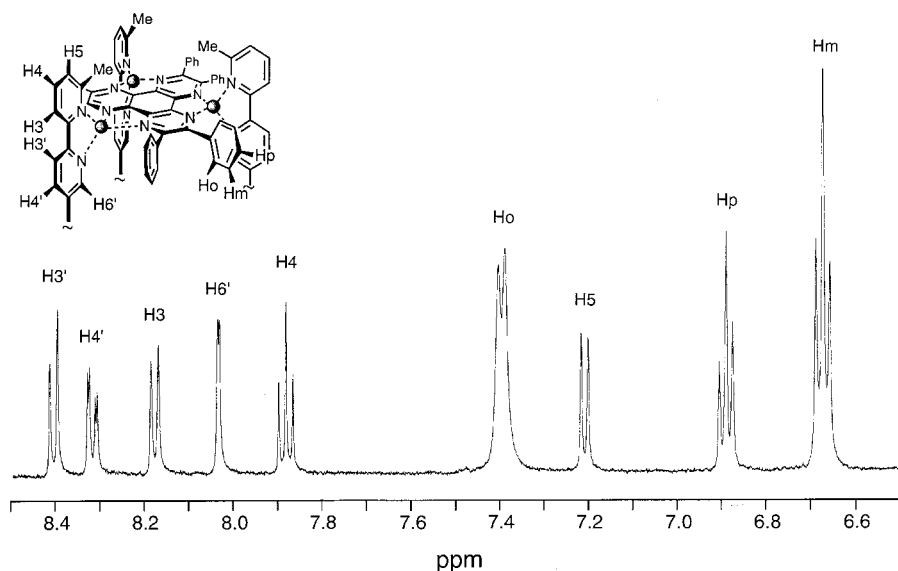


Figure 2.  $^1\text{H}$  NMR spectrum of complex **1b** at 500 MHz in  $\text{CD}_3\text{NO}_2$  (25 °C).

The silver(I)-containing analogue **1d** also formed in quantitative yield upon stirring a 1.5:1:3 stoichiometric ratio of **7a**, **8**, and  $\text{AgCF}_3\text{SO}_3$  in  $\text{MeNO}_2$  at ambient temperature for 24 h. Complex **1d** was characterised by  $^1\text{H}$  and  $^{13}\text{C}$  NMR spectroscopy, elemental analysis, and X-ray crystallography. The crystal structure revealed that the cation, unlike the helically twisted  $\text{Cu}^{\text{I}}$ -containing analogue **1b**, was shaped into an almost perfect trigonal prism (Figure 3). The complex is

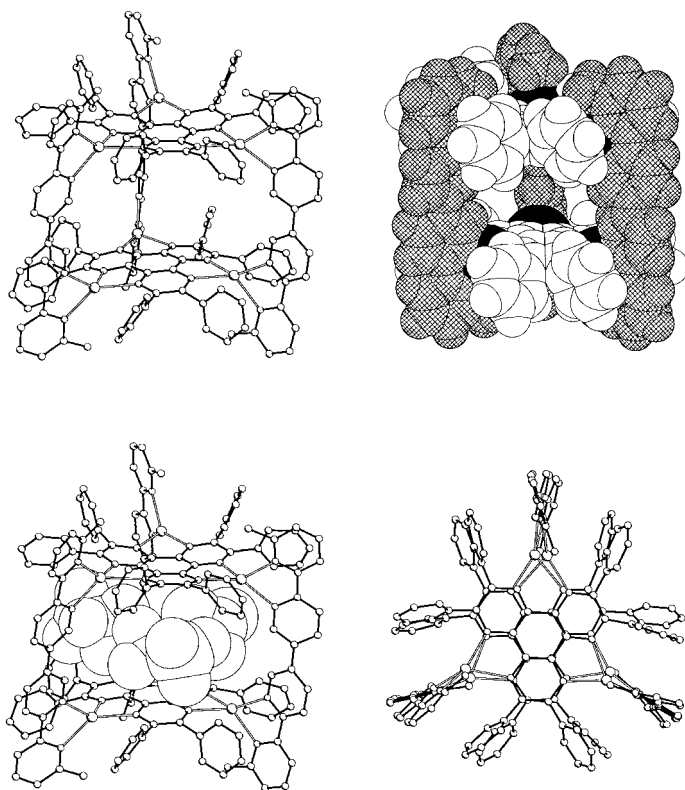


Figure 3. Representations of the crystal structure of the cylindrical cage complex **1d**: side view (top left), space-filling side view (top right) side view with included substrates, see text (bottom left), view along the axis of the cylinder (bottom right).

composed of three vertically positioned **7a** ligands forming the walls of the cage, closed top and bottom by two **8** ligands, and cemented together by six  $\text{Ag}^+$  ions. The distance between the  $\text{Ag}^+$  ions along the axis of **7a** is 8.16–8.26 Å, and 7.38–7.44 Å within the **8** mean planes. The bipyridine subunits of the **7a** ligands are slightly twisted from planarity, with a maximum deviation of 14.56° between the intra-subunit pyridine ring mean planes. The bipyridines are also twisted relative to each other with a maximum angle of 31.21° between their mean planes. The **8** ligand planes are however only

slightly rotated with respect to each other by 7.43° and are seen to be almost eclipsed when viewed down the long axis of **1d**. The small relative rotation between the **8** ligands results mainly from the inter-bipyridine twisting discussed above. The  $\text{Ag}-\text{N}$  bond lengths 2.284(7)–2.405(6) Å, and the  $\text{N}7\text{a}-\text{Ag}-\text{N}7\text{a}$  73.1(3)–74.0(3)°,  $\text{N}8-\text{Ag}-\text{N}8$  71.6(2)–72.2(2)°, and  $\text{N}7\text{a}-\text{Ag}-\text{N}8$  119.0(2)–140.1(2)° angles are representative of all  $\text{Ag}^+$  ions with partially distorted tetrahedral coordination polyhedra. The overall dimensions of the complex are 20.2 (height)  $\times$  19.4 (diameter) Å, which make it 1.2 Å longer and 0.6 Å narrower than the  $\text{Cu}^{\text{I}}$  analogue **1b**, due to the almost eclipsed conformation of **1d**. The cation **1d** possesses an internal cavity of 4.7 (height)  $\times$  9.2 (diameter) Å (taking Van der Waals radii into account) inside which are captured two triflate anions and a single  $\text{MeNO}_2$  solvent molecule. The guests are positioned in the same plane in such a way that almost all available space within the cavity is filled. Each guest species also partly protrudes through each of the three cavity portals into the antechambers defined by the **7a** ligand surfaces and the **8** phenyl rings.

These results demonstrate the generation of molecular cage-type architectures by metal ion-mediated multicomponent self-assembly. The next important question to be answered concerned the possibility of extending the approach to construct cages possessing different dimensions, in particular by increasing the length of the rigid linear component **7a**.

Having established the success of the above design principle in constructing inorganic cages, an important further question concerned the possibility of engineering the size and shape of the internal void within cations such as **1** in a predictable and controllable way. Such species would have the potential capacity for shape-selective and multiple-guest inclusion. Towards this goal, vertical elongation of the cage **1** was attempted by utilizing ligands structurally similar to **7a** but incorporating bridging groups between the bipyridine subunits, and repeating the reaction conditions which were successful for the self-assembly of **1a**.

**Self-assembly of the elongated cylindrical architectures 2–6 with rigid ligand bridges:** Cages possessing cylindrical cavities (2–6, see Scheme 1 and Figure 1) were prepared by using a class of ligand structurally similar to **7a** but axially elongated by the incorporation of rigidly preorganized bridges between the bipyridine subunits. Thus ligands **7b–f** were synthesized and each mixed with **8** and  $[\text{Cu}(\text{MeCN})_4]\text{PF}_6$  in a 1.5:1:3 ratio under the same experimental conditions as that used to prepare **1a**. Examination of the reaction mixtures by  $^1\text{H}$  NMR spectroscopy prior to workup revealed that the cylindrical complex **2** had formed in 50% yield, **3** and **4** in 90% – quantitative yield and **5** and **6** in 60–80% yield. There exists therefore a correlation between the efficiency of the self-assembly and the presence or absence of acetylene groups in the reacting components. The presence of acetylenic functions has a deleterious effect upon the yields of **2**, **5**, and **6**. The reason for this may be related to the enhanced chemical reactivity of the acetylene bridges compared to the phenyl spacers. Complexes **2–6** were characterised on the basis of elemental analysis,  $^1\text{H}$ , and  $^{13}\text{C}$  NMR, and UV/Vis spectroscopy, and ES mass spectrometry. The  $^1\text{H}$  and  $^{13}\text{C}$  NMR spectra of **2–6** indicated the presence of a highly symmetrical species in solution with ligands **7b–f** and **8** in a single magnetic and chemical environment. The signals observed agree with the cylindrical structures **2–6** (see Experimental Section). Figure 4 illustrates the  $^1\text{H}$  NMR spectrum of complex **5**. In the complexes elongated by means of acetylene containing bridges (**2**, **5**, **6**), the band corresponding to the *ortho* phenyl ring protons of **8** appeared as a sharp doublet. This is consistent with an unrestricted movement of anions through the larger portals in the walls of these complexes (see also below). The ES mass spectra showed bands assignable to the cylindrical complexes with successive loss of 2–6  $\text{PF}_6^-$  counterions.

Thus, rigid preorganization of both reacting ligand species proved to be a successful design modification for generating cylindrical cages with a range of cavity sizes. Molecular

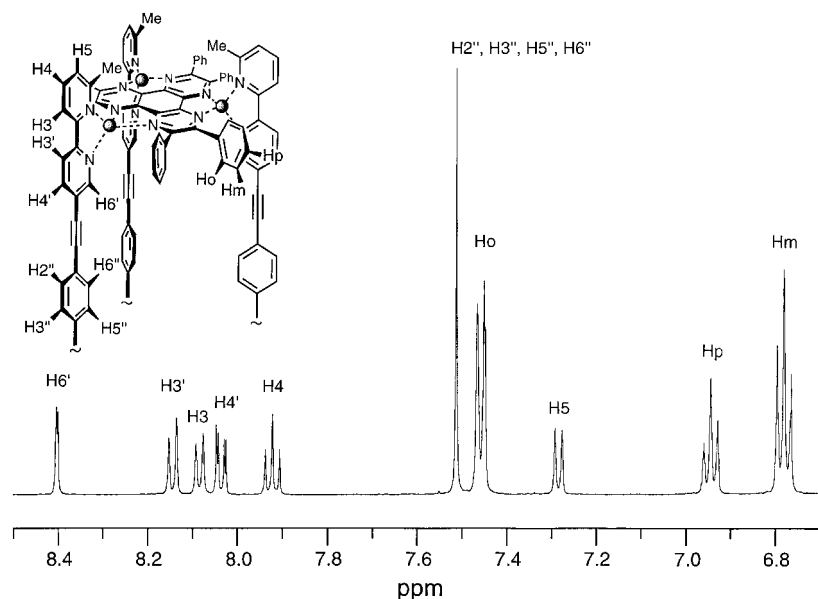


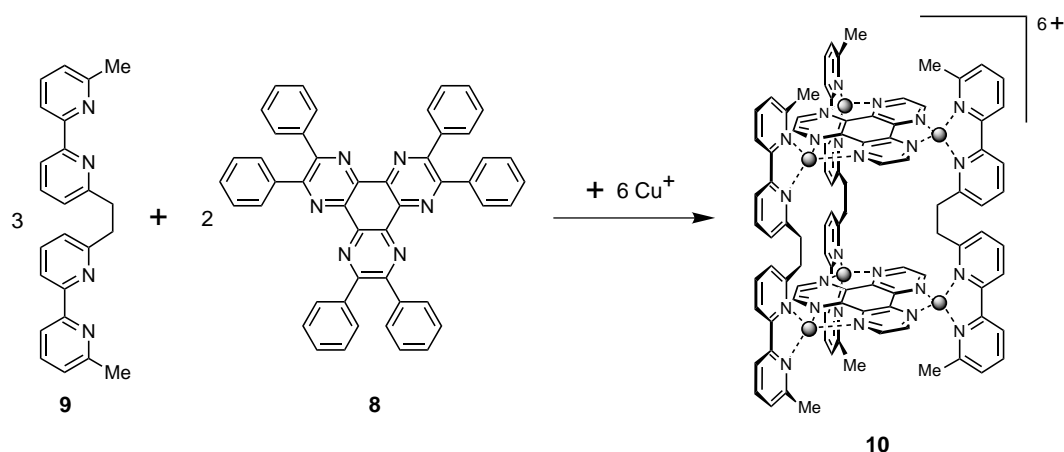
Figure 4.  $^1\text{H}$  NMR spectrum of complex **5** at 500 MHz in  $\text{CD}_3\text{NO}_2$  (25 °C).

modeling of **6** showed the external dimensions of the complex to be 33 (height)  $\times$  20 (diameter) Å in the extended non-helical conformation.<sup>[16]</sup> Complex **6** is therefore a truly nanoscopic cylinder which has been designed and generated through a multicomponent self-assembly strategy.

**Self-assembly of the cylindrical architecture 10 with conformationally flexible ligand bridges:** During initial attempts at generating cages with cylindrical cavities, bisbipyridines functionalized in the 5 and 6 pyridine ring positions with flexible bridges such as  $\text{CH}_2\text{-O-CH}_2$  and  $(\text{CH}_2)_n$  ( $n=6-14$ ) were used in place of **7a**. All reactions failed to yield isolable quantities of the cages even after prolonged reaction times and elevated temperatures. A  $^1\text{H}$  NMR spectroscopic investigation of the reactions in a variety of solvents showed only a complex mixture of unidentified and interconverting species. However, it was encouraging that no formation of insoluble polymers was observed.

Cage complex **10** was isolated from the reaction of a 1.5:1:3 ratio of **9**,<sup>[17]</sup> **8**, and  $[\text{Cu}(\text{MeCN})_4]\text{PF}_6$  in  $\text{MeNO}_2$  (Scheme 2). The  $^1\text{H}$  NMR spectrum of the reaction solution in  $\text{CD}_3\text{NO}_2$  and  $\text{CD}_2\text{Cl}_2$  prior to workup showed a considerable degree of complexity indicative of the presence of multiple species in slow to medium exchange on the NMR timescale. An ES mass spectrum of the reaction mixture in  $\text{CH}_2\text{Cl}_2$  at  $10^{-4}$  mol dm $^{-3}$  showed **10** to be the dominant species in solution, accompanied by lesser amounts of  $[\text{Cu}_2(\mathbf{9})_2]^{2+}$  and  $[\text{Cu}(\mathbf{8})_2]^+$ . Diffusion of an excess of diisopropyl ether into the reaction mixture resulted in the formation of a high yield of crystalline **10**. Complex **10** therefore appears to be most stable in the solid state, and can be selectively isolated from the mixture by simple adjustment of the reaction conditions (i.e. adding a precipitating solvent).<sup>[18]</sup>

An X-ray crystal structure determination was performed on the above reaction product and confirmed its identity as the cage complex **10**. The cation is shaped into a highly twisted helical cage in which two **8** ligands form the top and bottom, respectively, and three **9** ligands, the walls of the complex (Figure 5). The ligand components are held together by six  $\text{Cu}^+$  ions which are each separated by an average of 6.87 Å within the **8** planes and 7.65 Å between the **8** planes. The overall dimensions of the complex are 19.0 (height)  $\times$  20.0 (diameter) Å which make it identical in size to **1b**. The almost planar **8** ligands are slightly warped in shape with maximum deviations of +0.10 to  $-0.13$  Å from their mean planes. They are also staggered relative to each other by 20.1° as viewed down the long axis of the complex. In order to minimize strain within the bridging ethylene groups and orient the nitrogen lone



Scheme 2. Multicomponent self-assembly of the cylindrical architecture **10** from the linear flexible **9** and circular **8** ligands and copper(I) cations; phenyl rings of **8** in **10** omitted for clarity.

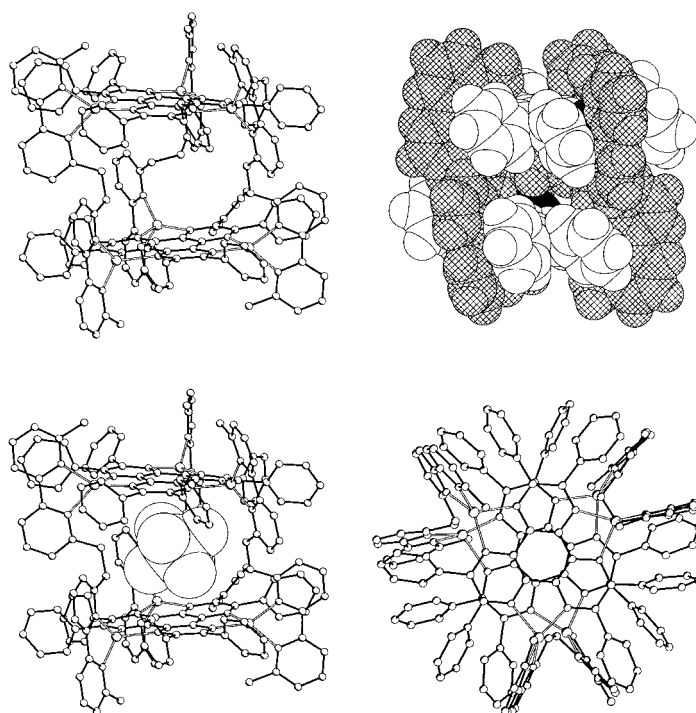


Figure 5. Representations of the crystal structure of the cylindrical cage complex **10**: side view (top left), space-filling side view (top right) side view with included  $\text{PF}_6^-$  ion, (bottom left), view along the axis of the cylinder (bottom right).

pairs towards the central axis of the cage, the bipyridine subunits have had to become laterally displaced from each other within each **9** ligand by a maximum distance of 4–5 Å between their mean planes and also rotated with respect to each other by 33.5–67.2°. As viewed down the axes of the **9** ligands, the bipyridine mean planes do not symmetrically bisect the Cu–**8** chelate rings, but are all tilted by 4–27° to one side and in the same directional sense within each **8** ligand, and in a clockwise–anticlockwise relationship between each **8** plane. The Cu–N bond lengths of 1.991(3)–2.185(3) Å, and N**9**–Cu–N**9** 81.7(2)–83.0(2)°, N**8**–Cu–N**8** 81.7(1)–82.6(1)°, and N**8**–Cu–N**9** 103.8(1)–137.1(2)° angles are representative of all  $\text{Cu}^+$  ions in a distorted tetrahedral coordination geometry.

Complex **10** is helically twisted to a greater degree than **1b**. This could be due to the summed effects of the distorted tetrahedral coordination polyhedra of the six  $\text{Cu}^+$  ions and the twisted conformation of the three **9** ligands. Inside the cage is a small cavity of dimensions 4.5 (height) × 5.5 (diameter) Å (taking Van der Waals radii into account) which is occupied by a single  $\text{PF}_6^-$  ion with an almost perfect fit. The contracted diameter of the cavity of **10** relative to **1b** results directly from the steric volume imposed by the internally facing bridging ethylene groups of the three **9** ligands.

**Ligand selection in the self-assembly of inorganic cages:** In order to explore the degree to which recognition can operate within a complex mixture, an experiment was performed in which a 1:1:1:3:6 stoichiometric combination of respectively **7a**:**7c**:**7d**:**8**: $[\text{Cu}(\text{MeCN})_4]\text{PF}_6$  was allowed to stir in nitromethane for 72 h. Analysis of the resulting purple solution by  $^1\text{H}$  NMR spectroscopy and ES mass spectrometry showed that only three species were present in solution, that is the cage complexes **1a**, **3**, and **4**. This result represents a remarkable example of correct recognition fidelity within a combinatorial library of self-assembling entities, based on four different ligands and involving a total of 33 particles (15 ligand molecules and 18 copper(I) ions) which associate with correct recognition, propagation, and termination to yield three structurally complex supermolecules. Previous studies with helicate mixtures<sup>[19]</sup> showed that only products comprising identical ligand strands were formed through a process of self-recognition. In the above example many more particles are initially present within the reaction mixture and the products form only by recognition between ligands of different identity. This situation which is of a higher information content, may be termed as nonself-recognition, and bears analogy to biological phenomena as found for instance in the immune system.

**Self-assembly and properties:** The above results demonstrate that it is possible to utilize a multicomponent strategy as a design principle for the metal-ion-directed self-assembly of complex three-dimensional molecular architectures of nanoscopic dimensions. In the multicomponent approach,  $\geq$  two ligand types correctly associate along with the metal ions to

yield the desired supermolecule.<sup>[20a–k]</sup> The self-assembly of cations **1** proceeded with a very high level of efficiency as all complexes investigated were found to form in high to quantitative yield prior to workup. The Ag<sup>+</sup> ion mediated self-assembly resulted in quantitative formation of **1d**. This presumably originates from the fact that Ag–N(bipyridine) bonds are weaker than the Cu–N(bipyridine) analogues, as evidenced by the lower stability constants of [Ag(2,2'-bipy)<sub>2</sub>]<sup>+</sup>-type complexes in donating solvents. This in turn would allow an increased Ag–N bond-forming/dissociation reversibility (error checking) and thus a more facile pathway to the final closed structure.

The effect of anions upon the self-assembly of **1** was also investigated. The formation of **1a**, **1b** and **1c** proceeded in quantitative yield in the presence of PF<sub>6</sub><sup>-</sup>, BF<sub>4</sub><sup>-</sup> and ClO<sub>4</sub><sup>-</sup> counterions, respectively. However, when the self-assembly of **1** was attempted with CuCl and CuBr in MeCN/H<sub>2</sub>O mixtures, no evidence for the formation of the cages was observed after 48 h at ambient temperature. Slow decomposition also occurred when (*n*Bu)<sub>4</sub>NX salts (X = Cl<sup>-</sup>, Br<sup>-</sup>) were added to preformed **1a** in MeNO<sub>2</sub> solution. The formation of **1** appears therefore to be strongly influenced by the class of anion. The failure of the self-assembly in the presence of halogen anions may possibly be attributed to the propensity of Cu<sup>I</sup> to form halogen-bridged metal dimers, which in the absence of strong metal–bipyridine-type ligand binding would direct the reaction pathway to different products.<sup>[21]</sup> When Cu<sup>I</sup> salts of aromatic anions such as B(Ph)<sub>4</sub><sup>-</sup> and toluenesulfonate were employed, only insoluble precipitates were obtained. Also addition of the N(*n*Bu)<sub>4</sub><sup>+</sup> salts of the above anions to solutions of **1a** resulted in rapid precipitation of the respective complexes in MeNO<sub>2</sub> and MeCN. This may originate from the formation of extended aromatic contacts between the surface of the cations and the phenyl rings of the anions, thereby reinforcing and stabilising the resulting crystal lattice. The <sup>1</sup>H NMR spectra of complexes **1a–c** showed small differences between the chemical shifts of some of the externally positioned protons, suggesting that the anions are positioned in proximity to the Cu<sup>+</sup> ions in interligand pockets on the surface of the complexes and thereby influence the chemical shifts of closely situated protons.

The crystal structure of the Cu<sup>I</sup> complex **1b** shows the cation to be twisted into a helical conformation. The helical twisting is in accordance with the well documented preference of Cu<sup>I</sup> to adopt a distorted tetrahedral coordination polyhedron in the presence of bipyridine-type ligands.<sup>[22a–c]</sup> However, the crystal structure of the Ag<sup>I</sup> complex **1d**, is essentially non-helical, with an overall trigonal-prismatic shape. An X-ray crystallographic investigation of the structures of [M(L)<sub>2</sub>]<sup>+</sup> (M = Cu<sup>+</sup>, Ag<sup>+</sup>; L = bipyridine and phenanthroline ligands) complexes has revealed that the distortions from ideal tetrahedral coordination geometry in the solid-state result primarily from crystal packing factors.<sup>[22a–c, 23]</sup> The helical conformation of **1b** may result therefore from an attempt to minimise the cavity volume to best fit the guests and maximise intra- and intermolecular aromatic π–π interactions as well as to accommodate interstitial anions and solvent.

The <sup>1</sup>H NMR spectra of complexes **1a–d** show the bands assignable to the *ortho*-phenyl ring protons of the **8** ligands to

be considerably line broadened. This phenomenon appears to be linked to the presence of anions in the cage cavity.<sup>[24]</sup>

The cage complexes described here exhibit unusual and interesting physicochemical properties which are not expressed by their component parts, the anion guest inclusion discussed above being one example. Another example is the strikingly deep purple colour of the Cu<sup>I</sup> complexes which may hint to interesting photophysical properties. The colour originates from two metal-to-ligand charge transfer (MLCT) envelopes in the visible spectrum of the cages and is associated with the mixed ligand [Cu(**7a**)(**8**)]<sup>+</sup> chromophore. The Ag<sup>I</sup> complexes are unusual in that they are stable to light, even upon exposure for one year on the bench. The robust nature of these materials will be an attractive feature in any future applications.

## Conclusions

The above work describes the construction of a range of three-dimensional inorganic molecular architectures of cylindrical shape and nanometric size (Figure 1). The principle for their design consists of a metal-ion-mediated multicomponent self-assembly process in which ligands of different identity preferentially combine in the presence of metal ions to generate the desired closed structure. The multicomponent approach represents a highly convergent type of self-assembly of greater information content than systems comprising metal ions and single ligand species, and which in principle should be capable of accessing the highest levels of structural complexity at the molecular level in the shortest number of steps. The success of this strategy relies upon two main factors; i) that the metal-ion–ligand bonding interactions are reversible and that the reaction proceeds under equilibrium thermodynamic control, and ii) the ligands are designed in such a way as to destabilise the formation of polymers and stabilise the desired supramolecular product. In the latter case the use of rigidly preorganised ligands functionalised with sterically hindering groups was found to be of crucial importance to the success of the self-assembly. The phenyl rings of **8** were chosen in order to fulfill the above requirements by reducing the degree to which **8** can polymerise in the presence of metal ions through steric interactions and to stabilise the resulting cage structure through multiple attractive intramolecular contacts.<sup>[14, 25]</sup>

All cage complexes possess an average C<sub>3</sub> symmetric architecture laterally expanded to provide an internal cavity. A high level of control over the cavity size and shape was achieved by using rigidly preorganised ligand components which allowed the construction of internal voids varying in size from Ångstrom (**1a–d**) to nanoscopic dimensions (**2–6**). The self-assembled complexes also fulfill the expectation of displaying physicochemical properties not expressed by their component parts such as anion guest inclusion behaviour. They can therefore be regarded as metallocryptands which are accessible through self-assembly and do not require lengthy sequential synthetic protocols and low yield statistical cyclisation reactions for their construction.

The present results demonstrate that it is possible to access in a single overall step supramolecular architectures of

nanometric size presenting a high level of structural complexity by metal-ion-mediated self-assembly. The formation of the cage complexes results from the operation of a programmed, informational process that involves three main stages: a) initiation, b) propagation, and finally c) termination of the assembly leading to a discrete supermolecule. Entropic and solvation factors are also expected to play an important role in the generation of such species.

Other extensions of the above work currently under investigation include further alteration of the cavity size and shape, extension to octahedral metal ion analogues, incorporation into higher order structures and surface chemical studies, as well as self-assembly of multicompartamental architectures from polytopic components.<sup>[27]</sup>

## Experimental Section

**General techniques:** The metal-ion containing salts  $[\text{Cu}(\text{CH}_3\text{CN})_4]\text{PF}_6$  and  $\text{AgCF}_3\text{SO}_3$  were purchased from Aldrich. The former was recrystallised from MeCN and the latter from benzene prior to use. The solvents nitrobenzene and nitromethane (Fluka, puriss) were redistilled under vacuum before use. Adsorption column chromatography was performed using silica gel (GEDURAN, SI 60 (40–63  $\mu\text{m}$ , MERCK). Ligands **7b–f** were prepared by using standard organometallic coupling protocols.<sup>[26]</sup> Ultraviolet/visible spectra were recorded on a Varian, CARY 3 spectrophotometer in  $\text{CH}_2\text{Cl}_2$  redistilled from  $\text{CaH}_2$  under argon. Infrared spectra were recorded as compressed KBr discs on a Perkin Elmer 1600 Series FTIR. The following notation is used for the IR spectral intensities; strong (s), medium (m), weak (w), shoulder (sh). 500 MHz  $^1\text{H}$  and 125 MHz  $^{13}\text{C}$  NMR spectra were recorded on a Bruker ARX 500 spectrometer and 300 MHz  $^1\text{H}$  and 75 MHz  $^{13}\text{C}$  NMR spectra on a Bruker AM 300 spectrometer, and were referenced to residual  $\text{CH}_3\text{NO}_2$  in the  $\text{CD}_3\text{NO}_2$  solvent. ES-MS studies were performed on a VG BioQ triple quadrupole mass spectrometer upgraded in order to obtain the Quattro II performances (Micromass, Altrincham, UK). Samples were dissolved in  $\text{MeNO}_2$  at  $10^{-4}$ – $10^{-5}\text{M}$  and were continuously infused into the ion source at a flow rate of 6 mL  $\text{min}^{-1}$ , via a Harvard Model 55 1111 syringe pump (Harvard Apparatus, South Natick, MA, USA). The extraction cone voltage (Vc) was at 20 V to avoid fragmentations. Elemental analyses were performed by the Service de Microanalyse, Institut de Chimie, Université Louis Pasteur.

**General procedure for 1a–c:** Nitromethane (2 mL) was added by syringe to a 1.5:1 stoichiometric mixture of **7a** and **8** under an atmosphere of argon. A solution of three equivalents of  $[\text{Cu}(\text{CH}_3\text{CN})_4]\text{X}$  in acetonitrile (1.5 mL) was then added by syringe, and the mixture stirred at ambient temperature for 48 h. All solvent was then removed from the purple solution under vacuum and the remaining solid dissolved in nitromethane (3 mL), gravity-filtered and benzene added dropwise over 2 h until formation of solid ceased. The solid was isolated by filtration under vacuum, washed with benzene, air dried and further dried under vacuum at  $85^\circ\text{C}/2 \times 10^{-6}\text{ mmHg}$ .

**1a:** From **7a** (0.0184 g,  $5.43 \times 10^{-5}\text{ mol}$ ), **8** (0.025 g,  $3.62 \times 10^{-5}\text{ mol}$ ) and  $[\text{Cu}(\text{CH}_3\text{CN})_4](\text{PF}_6)$  (0.0405 g,  $1.09 \times 10^{-4}\text{ mol}$ ) was obtained **1a** (0.064 g, 97%) as permanganate-coloured microcrystals, which were considered pure by  $^1\text{H}$  and  $^{13}\text{C}$  NMR spectroscopy and ES mass spectrometry. Microanalytically pure material was however only obtained upon further purification by flash chromatography through a short plug of silica, eluting with 1%  $\text{MeOH}/\text{CH}_2\text{Cl}_2$  then then 4%  $\text{MeOH}/\text{CH}_2\text{Cl}_2$  followed by recrystallisation from  $\text{CH}_2\text{Cl}_2$ /benzene and finally drying under vacuum at  $100^\circ\text{C}/0.1\text{ mmHg}$ .  $^1\text{H}$  NMR ( $\text{CD}_3\text{NO}_2$ , 500 MHz,  $25^\circ\text{C}$ ):  $\delta = 8.43$  (d,  $J_{3,4} = 8.6\text{ Hz}$ , 6H; **7aH-3'**), 8.30 (d,  $J_{4,3} = 7.9\text{ Hz}$ , 6H; **7aH-4'**), 8.22 (d,  $J_{3,4} = 8.0\text{ Hz}$ , 6H; **7aH-3**), 8.04 (s, 6H; **7aH-6'**), 7.88 (t,  $J_{4,3,4,5} = 7.9\text{ Hz}$ , 6H; **7aH-4**), 7.40 (s, 24H; **8H-ortho**), 7.17 (d,  $J_{3,4} = 7.7\text{ Hz}$ , 6H; **7aH-5**), 6.89 (t,  $J_{\text{p,m}} = 7.4\text{ Hz}$ , 12H; **8H-para**), 6.68 (t,  $J_{\text{m,o,m,p}} = 7.4\text{ Hz}$ , 24H; **8H-meta**), 2.15 (s, 18H; **7a-CH}\_3**);  $^{13}\text{C}$  NMR ( $\text{CD}_3\text{NO}_2$ , 125.8 MHz,  $25^\circ\text{C}$ ):  $\delta = 159.02$ , 157.64,

153.10, 151.67, 147.04, 140.40, 140.15, 138.23, 138.12, 134.78, 131.57, 130.66, 129.00, 127.73, 124.57, 121.37; 26.17 ( $\text{CH}_3$ ). ES MS ( $\text{CH}_3\text{NO}_2$ ):  $m/z$  (relative intensity, %): 1679.1 (3)  $[\{\text{Cu}_6(\mathbf{7a})_3(\mathbf{8})_2\}(\text{PF}_6)_4]^{2+}$ , 1071.1 (11)  $[\{\text{Cu}_6(\mathbf{7a})_3(\mathbf{8})_2\}(\text{PF}_6)_3]^{3+}$ , 767.0 (34)  $[\{\text{Cu}_6(\mathbf{7a})_3(\mathbf{8})_2\}(\text{PF}_6)_2]^{4+}$ , 584.7 (100)  $[\{\text{Cu}_6(\mathbf{7a})_3(\mathbf{8})_2\}(\text{PF}_6)]^{5+}$ ; UV/Vis ( $\text{CH}_2\text{Cl}_2$ ):  $\lambda$  [nm] ( $\epsilon$  [ $\text{mol}^{-1}\text{dm}^3\text{cm}^{-1}$ ]): 287 (119785), 338 (211647), 383 (111096), 546 (27678), 695 (12977); elemental analysis calcd. for  $\text{C}_{162}\text{H}_{114}\text{Cu}_6\text{F}_{36}\text{N}_{24}\text{P}_6$  (%): C 53.34, H 3.15, N 9.22; found C 53.15, H 3.30, N 9.35.

**1b:** From **7a** (0.0184 g,  $5.43 \times 10^{-5}\text{ mol}$ ), **8** (0.025 g,  $3.62 \times 10^{-5}\text{ mol}$ ) and  $[\text{Cu}(\text{CH}_3\text{CN})_4](\text{BF}_4)$  (0.0342 g,  $1.09 \times 10^{-4}\text{ mol}$ ) was obtained **1b** (0.058 g, 97%) as permanganate-coloured microcrystals, which were considered pure by  $^1\text{H}$  and  $^{13}\text{C}$  NMR spectroscopy and ES mass spectrometry. Microanalytically pure material was obtained by column chromatography, recrystallisation and drying as described for **1a** above.  $^1\text{H}$  NMR ( $\text{CD}_3\text{NO}_2$ , 500 MHz,  $25^\circ\text{C}$ ):  $\delta = 8.41$  (d,  $J_{3,4} = 8.8\text{ Hz}$ , 6H; **7aH-3'**), 8.32 (dd,  $J_{4,3} = 8.7\text{ Hz}$ ,  $J_{4,6} = 2.2\text{ Hz}$ , 6H; **7aH-4'**), 8.18 (d,  $J_{3,4} = 8.1\text{ Hz}$ , 6H; **7aH-3**), 8.03 (d,  $J_{6,4} = 1.8\text{ Hz}$ , 6H; **7aH-6'**), 7.88 (t,  $J_{4,3,4,5} = 7.9\text{ Hz}$ , 6H; **7aH-4**), 7.40 (d,  $J_{\text{o,m}} = 7.2\text{ Hz}$ , 24H; **8H-ortho**), 7.21 (d,  $J_{3,4} = 7.8\text{ Hz}$ , 6H; **7aH-5**), 6.89 (t,  $J_{\text{p,m}} = 7.5\text{ Hz}$ , 12H; **8H-para**), 6.67 (t,  $J_{\text{m,o,m,p}} = 7.8\text{ Hz}$ , 24H; **8H-meta**), 2.16 (s, 18H; **7a-CH}\_3**); UV/Vis ( $\text{CH}_2\text{Cl}_2$ ):  $\lambda$  [nm] ( $\epsilon$  [ $\text{mol}^{-1}\text{dm}^3\text{cm}^{-1}$ ]): 287 (125789), 339 (221517), 382 (115652), 545 (28792), 694 (13969); elemental analysis calcd. for  $\text{C}_{162}\text{H}_{114}\text{B}_6\text{Cu}_6\text{F}_{24}\text{N}_{24}$  (%): C 58.98, H 3.48, N 10.19; found C 58.74, H 3.28, N 9.99.

**1c:** From **7a** (0.0194 g,  $5.73 \times 10^{-5}\text{ mol}$ ), **8** (0.0264 g,  $3.82 \times 10^{-5}\text{ mol}$ ) and  $[\text{Cu}(\text{CH}_3\text{CN})_4](\text{ClO}_4)$  (0.0375 g,  $1.15 \times 10^{-4}\text{ mol}$ ) was obtained **1c** (0.057 g, 89%) as a permanganate-coloured powder, pure by  $^1\text{H}$ ,  $^{13}\text{C}$  NMR spectroscopy and ES mass spectrometry. Microanalytically pure material was obtained by column chromatography, recrystallisation and drying as described for **1a**.  $^1\text{H}$  NMR ( $\text{CD}_3\text{NO}_2$ , 500 MHz,  $25^\circ\text{C}$ ):  $\delta = 8.40$  (d,  $J_{3,4} = 8.6\text{ Hz}$ , 6H; **7aH-3'**), 8.30 (dd,  $J_{4,3} = 8.7\text{ Hz}$ ,  $J_{4,6} = 2.2\text{ Hz}$ , 6H; **7aH-4'**), 8.18 (d,  $J_{3,4} = 8.1\text{ Hz}$ , 6H; **7aH-3**), 8.05 (d,  $J_{6,4} = 2.0\text{ Hz}$ , 6H; **7aH-6'**), 7.88 (t,  $J_{4,3,4,5} = 7.9\text{ Hz}$ , 6H; **7aH-4**), 7.41 (d,  $J_{\text{o,m}} = 6.8\text{ Hz}$ , 24H; **8H-ortho**), 7.20 (d,  $J_{3,4} = 7.7\text{ Hz}$ , 6H; **7aH-5**), 6.88 (t,  $J_{\text{p,m}} = 7.6\text{ Hz}$ , 12H; **8H-para**), 6.67 (t,  $J_{\text{m,o,m,p}} = 7.8\text{ Hz}$ , 24H; **8H-meta**), 2.17 (s, 18H; **7a-CH}\_3**); UV/Vis ( $\text{CH}_2\text{Cl}_2$ ):  $\lambda$  [nm] ( $\epsilon$  [ $\text{mol}^{-1}\text{dm}^3\text{cm}^{-1}$ ]): 288 (130307), 339 (239217), 383 (124772), 545 (31374), 698 (15039); elemental analysis calcd. for  $\text{C}_{162}\text{H}_{114}\text{Cl}_6\text{Cu}_6\text{N}_{24}\text{O}_{24}$  (%): C 57.66, H 3.40, N 9.96; found: C 57.48, H 3.49, N 9.75.

**1d:** To a mixture of **7a** (0.015 g,  $4.43 \times 10^{-5}\text{ mol}$ ), **8** (0.020 g,  $2.95 \times 10^{-5}\text{ mol}$ ) and  $\text{AgCF}_3\text{SO}_3$  (0.023 g,  $8.87 \times 10^{-5}\text{ mol}$ ) was added nitromethane (2 mL), the mixture briefly ultrasonicated, then left to stir at ambient temperature for 24 h. All solvent was removed under vacuum and the remaining solid washed with benzene. The product was then recrystallised by adding excess benzene to a solution of the complex in nitromethane over a 2 h period. Isolation by vacuum filtration, washing with benzene and drying under vacuum ( $85^\circ\text{C}/2 \times 10^{-6}\text{ mmHg}$ ) yielded **1d** (0.057 g, 98%) as yellow microcrystals.  $^1\text{H}$  NMR ( $\text{CD}_3\text{NO}_2$ , 500 MHz,  $25^\circ\text{C}$ ):  $\delta = 8.37$  (dd,  $J_{4,3} = 8.7\text{ Hz}$ ,  $J_{4,6} = 2.3\text{ Hz}$ , 6H; **7aH-4'**), 8.34 (d,  $J_{3,4} = 8.4\text{ Hz}$ , 6H; **7aH-3'**), 8.20 (d,  $J_{3,4} = 8.0\text{ Hz}$ , 6H; **7aH-3**), 8.17 (s, 6H; **7aH-6'**), 7.97 (t,  $J_{4,3,4,5} = 7.9\text{ Hz}$ , 6H; **7aH-4**), 7.55 (d,  $J_{\text{o,m}} = 6.9\text{ Hz}$ , 24H; **8H-ortho**), 7.25 (d,  $J_{3,4} = 8.1\text{ Hz}$ , 6H; **7aH-5**), 6.86 (t,  $J_{\text{p,m}} = 7.6\text{ Hz}$ , 12H; **8H-para**), 6.70 (t,  $J_{\text{m,o,m,p}} = 7.7\text{ Hz}$ , 24H; **8H-meta**), 2.15 (s, 18H; **7a-CH}\_3**);  $^{13}\text{C}$  NMR ( $\text{CD}_3\text{NO}_2$ , 125.7 MHz,  $25^\circ\text{C}$ ):  $\delta = 160.21$ , 158.94, 152.95, 152.10, 148.57, 140.79, 139.74, 139.46, 137.96, 134.10, 132.02, 130.60, 129.57, 127.03, 125.06, 121.94, 27.35 ( $\text{CH}_3$ ), {126.29, 123.74, 121.18, 118.63  $\text{CF}_3\text{SO}_3$ }; UV/Vis ( $\text{CH}_2\text{Cl}_2$ ):  $\lambda$  [nm] ( $\epsilon$  [ $\text{mol}^{-1}\text{dm}^3\text{cm}^{-1}$ ]): 333 (220522), 376 (91273); elemental analysis calcd. for  $\text{C}_{168}\text{H}_{114}\text{Ag}_6\text{F}_{18}\text{N}_{24}\text{O}_{18}\text{S}_6$  (%): C 51.23, H 2.92, N 8.54; found: C 51.29, H 2.98, N 8.57.

**10:** To a mixture of **9** (0.0162 g,  $4.42 \times 10^{-5}\text{ mol}$ ), **8** (0.0204 g,  $2.95 \times 10^{-5}\text{ mol}$ ) and  $[\text{Cu}(\text{CH}_3\text{CN})_4](\text{PF}_6)$  (0.033 g,  $8.85 \times 10^{-5}\text{ mol}$ ) under argon, was added nitromethane (2 mL) by syringe. The reaction was stirred at ambient temperature for 24 h, during which time the colour changed from brown through black-green to finally deep blue. The solvent was then removed under vacuum and the remaining solid recrystallised from nitromethane-diisopropyl ether by liquid–liquid diffusion. The product was isolated by filtration under vacuum, washed with diisopropyl ether, air dried and further dried at  $100^\circ\text{C}/2 \times 10^{-6}\text{ mmHg}$  to yield **10** (0.045 g, 82%) as blue-black crystals. ES MS ( $\text{CH}_2\text{Cl}_2$ ):  $m/z$  (relative intensity, %): 1721.3 (46)  $[\{\text{Cu}_6(\mathbf{9})_3(\mathbf{8})_2\}(\text{PF}_6)_4]^{2+}$ , 1445.2 (19)  $[\text{Cu}(\mathbf{8})_2]^{+}$ , 1099.1 (69)  $[\{\text{Cu}_6(\mathbf{9})_3(\mathbf{8})_2\}(\text{PF}_6)_3]^{3+}$ , 788.2 (100)  $[\{\text{Cu}_6(\mathbf{9})_3(\mathbf{8})_2\}(\text{PF}_6)_2]^{4+}$ , 601.5 (75)  $[\{\text{Cu}_6(\mathbf{9})_3(\mathbf{8})_2\}(\text{PF}_6)]^{5+}$ , 429.9 (4)  $[\text{Cu}_2(\mathbf{9})_2]^{2+}$ .



**General procedure for 2–6:** To a mixture of **7b–f**, **8** and  $[\text{Cu}(\text{CH}_3\text{CN})_4](\text{PF}_6)_2$  in a 1.5:1:3 stoichiometric ratio under an argon atmosphere was added nitromethane (3–4 mL) by syringe and the reaction stirred at ambient temperature for 48 h (**2**, **3**), 72 h (**4**, **5**), and 168 h (**6**). All solvent was removed under vacuum, the remaining solid dissolved in the minimum volume of dichloromethane and purified by gradient elution flash chromatography down a short column of silica with increasing ratios of methanol/dichloromethane. The product was then dissolved in nitromethane (3 mL) and recrystallised by slow addition of excess benzene or toluene over a 2 h period. The crystalline solid was isolated by filtration under vacuum, washed with benzene, air dried and further dried under vacuum at  $90^\circ\text{C}/2 \times 10^{-6}$  mmHg.

**2:** From **7b** (0.031 g,  $8.55 \times 10^{-5}$  mol), **8** (0.039 g,  $5.65 \times 10^{-5}$  mol) and  $[\text{Cu}(\text{CH}_3\text{CN})_4](\text{PF}_6)_2$  (0.064 g,  $1.72 \times 10^{-4}$  mol) was obtained a solid which was purified by chromatography using first 3% MeOH/ $\text{CH}_2\text{Cl}_2$ , then 8% MeOH/ $\text{CH}_2\text{Cl}_2$ . Finally recrystallisation from MeNO<sub>2</sub>/toluene yielded **2** (0.026 g, 25%) as a dark purple microcrystalline powder. <sup>1</sup>H NMR ( $\text{CD}_3\text{NO}_2$ , 500 MHz, 25 °C):  $\delta = 8.22$  (dd,  $J_{6,4} = 1.9$  Hz,  $J_{6,3} = 0.8$  Hz, 6H; **7bH-6'**), 8.19 (dd,  $J_{3,4} = 8.7$  Hz,  $J_{3,6} = 0.8$  Hz, 6H; **7bH-3'**), 8.12 (dd,  $J_{4,3} = 8.5$  Hz,  $J_{4,6} = 2.0$  Hz, 6H; **7bH-4'**), 8.10 (d,  $J_{3,4} = 8.0$  Hz, 6H; **7bH-3**), 7.92 (t,  $J_{4,3,4,5} = 7.9$  Hz, 6H; **7bH-4**), 7.44 (dd,  $J_{\text{om}} = 8.3$  Hz,  $J_{\text{op}} = 1.1$  Hz, 24H; **8H-ortho**), 7.28 (d,  $J_{5,4} = 7.6$  Hz, 6H; **7bH-5**), 6.96 (tt,  $J_{\text{pm}} = 7.6$  Hz,  $J_{\text{po}} = 1.2$  Hz, 12H; **8H-para**), 6.82 (t,  $J_{\text{m,om,p}} = 7.9$  Hz, 24H; **8H-meta**), 2.21 (s, 18H; **7b-CH<sub>3</sub>**); <sup>13</sup>C NMR ( $\text{CD}_3\text{NO}_2$ , 125.8 MHz, 25 °C):  $\delta = 159.12, 157.61, 152.71, 151.72, 151.45, 142.74, 140.60, 140.14, 138.35, 131.49, 130.51, 129.22, 127.57, 123.49, 122.52, 121.40, 91.37$  (C≡C), 26.18 (CH<sub>3</sub>); ES MS ( $\text{CH}_3\text{NO}_2$ ):  $m/z$  (relative intensity; %): 1715.7 (3)  $[[\text{Cu}_6(\mathbf{7b})_3(\mathbf{8})_2](\text{PF}_6)_4]^{2+}$ , 1095.2 (15)  $[[\text{Cu}_6(\mathbf{7b})_3(\mathbf{8})_2](\text{PF}_6)_3]^{3+}$ , 785.0 (44)  $[[\text{Cu}_6(\mathbf{7b})_3(\mathbf{8})_2](\text{PF}_6)_2]^{4+}$ , 598.9 (100)  $[[\text{Cu}_6(\mathbf{7b})_3(\mathbf{8})_2](\text{PF}_6)]^{5+}$ ; UV/Vis ( $\text{CH}_2\text{Cl}_2$ ):  $\lambda$  [nm] ( $\epsilon$  [ $\text{mol}^{-1}\text{dm}^3\text{cm}^{-1}$ ]): 299 (124924), 348 (277477), 366 (264897), 390 (126108), 553 (33429), 672 (15414); IR ( $[\text{cm}^{-1}]$ ):  $\tilde{\nu} = 3106$  w, 3059 m, 3028 w, 2956 w, 2925 w, 2854 w, 1625 m, 1602 m, 1560 m, 1495 m, 1461 s, 1372 s, 1295 w, 1273 w, 1251 m, 1236 m, 1210 m, 1182 m, 1147 m, 1102 w, 1075 w, 1030 m, 1017 m, 1000 w, 843 s, 802 m, 771 m, 761 m, 753 m, 722 m, 701 s, 610 m, 558 s; elemental analysis calcd. for  $\text{C}_{160}\text{H}_{114}\text{Cu}_6\text{F}_{36}\text{N}_{24}\text{P}_6$  (%): C 54.24, H 3.09, N 9.04; found: C 54.08, H 3.33, N 9.12.

**3:** From **7c** (0.035 g,  $8.44 \times 10^{-5}$  mol), **8** (0.039 g,  $5.65 \times 10^{-5}$  mol) and  $[\text{Cu}(\text{CH}_3\text{CN})_4](\text{PF}_6)_2$  (0.064 g,  $1.72 \times 10^{-4}$  mol) was obtained a solid which was purified by chromatography and recrystallisation as described for **2** above to yield **3** (0.075 g, 69%) as permanganate-coloured microcrystals. <sup>1</sup>H NMR ( $\text{CD}_3\text{NO}_2$ , 500 MHz, 25 °C):  $\delta = 8.60$  (s, 6H; **7cH-6'**), 8.25 (s, 12H; **7cH-3'**), 8.15 (d,  $J_{3,4} = 8.0$  Hz, 6H; **7cH-3**), 7.93 (t,  $J_{4,3,4,5} = 7.9$  Hz, 6H; **7cH-4**), 7.77 (s, 12H; **7c** central phenyl H-2'', 3'', 5'', 6''), 7.49 (d,  $J_{\text{om}} = 7.3$  Hz, 24H; **8H-ortho**), 7.25 (d,  $J_{5,4} = 7.7$  Hz, 6H; **7cH-5**), 6.95 (t,  $J_{\text{pm}} = 7.6$  Hz, 12H; **8H-para**), 6.77 (t,  $J_{\text{m,om,p}} = 7.9$  Hz, 24H; **8H-meta**), 2.16 (s, 18H; **7c-CH<sub>3</sub>**); <sup>13</sup>C NMR ( $\text{CD}_3\text{NO}_2$ , 75 MHz, 25 °C):  $\delta = 158.92, 157.73, 152.49, 152.16, 148.24, 140.51, 140.07, 138.70, 138.53, 137.80, 137.63, 131.32, 130.66, 129.07, 127.11, 123.85, 120.99, 26.03$  (CH<sub>3</sub>); ES MS ( $\text{CH}_3\text{NO}_2$ ):  $m/z$  (relative intensity, %): 1794.0 (3)  $[[\text{Cu}_6(\mathbf{7c})_3(\mathbf{8})_2](\text{PF}_6)_4]^{2+}$ , 1147.1 (28)  $[[\text{Cu}_6(\mathbf{7c})_3(\mathbf{8})_2](\text{PF}_6)_3]^{3+}$ , 824.1 (60)  $[[\text{Cu}_6(\mathbf{7c})_3(\mathbf{8})_2](\text{PF}_6)_2]^{4+}$ , 630.2 (100)  $[[\text{Cu}_6(\mathbf{7c})_3(\mathbf{8})_2](\text{PF}_6)]^{5+}$ ; UV/Vis ( $\text{CH}_2\text{Cl}_2$ ):  $\lambda$  [nm] ( $\epsilon$  [ $\text{mol}^{-1}\text{dm}^3\text{cm}^{-1}$ ]): 345 (242758), 388 (119741), 557 (30538), 681 (13740); elemental analysis calcd. for  $\text{C}_{180}\text{H}_{126}\text{Cu}_6\text{F}_{36}\text{N}_{24}\text{P}_6$  (%): C 55.77, H 3.28, N 8.67; found: C 55.89, H 3.37, N 8.83.

**4:** From **7d** (0.040 g,  $8.15 \times 10^{-5}$  mol), **8** (0.0375 g,  $5.43 \times 10^{-5}$  mol) and  $[\text{Cu}(\text{CH}_3\text{CN})_4](\text{PF}_6)_2$  (0.061 g,  $1.64 \times 10^{-4}$  mol) was obtained a solid which was purified by chromatography and recrystallisation as described for **2** above to yield **4** (0.085 g, 77%) as permanganate-coloured crystals. <sup>1</sup>H NMR ( $\text{CD}_3\text{NO}_2$ , 500 MHz, 25 °C):  $\delta = 8.61$  (d,  $J_{6,4} = 2.0$  Hz, 6H; **7dH-6'**), 8.26 (d,  $J_{3,4} = 8.4$  Hz, 6H; **7dH-3'**), 8.22 (dd,  $J_{4,3} = 8.5$  Hz,  $J_{4,6} = 2.1$  Hz, 6H; **7dH-4'**), 8.16 (d,  $J_{3,4} = 8.1$  Hz, 6H; **7dH-3**), 7.94 (t,  $J_{4,3,4,5} = 7.9$  Hz, 6H; **7dH-4**), 7.83 (d,  $J_{2',3',6',5'} = 8.6$  Hz, 12H; **7dJ<sub>3',2',5',6'</sub>**), 7.73 (d, biphenyl inner H-2'', 6'' = 8.6 Hz, 12H; **7d** biphenyl outer H-3'', 5''), 7.51 (d,  $J_{\text{om}} = 7.5$  Hz, 24H; **8H-ortho**), 7.28 (d,  $J_{5,4} = 7.7$  Hz, 6H; **7dH-5**), 6.97 (t,  $J_{\text{pm}} = 7.5$  Hz, 12H; **8H-para**), 6.79 (t,  $J_{\text{m,om,p}} = 7.9$  Hz, 24H; **8H-meta**), 2.21 (s, 18H; **7d-CH<sub>3</sub>**); <sup>13</sup>C NMR ( $\text{CD}_3\text{NO}_2$ , 75 MHz, 25 °C):  $\delta = 158.91, 157.72, 152.17, 152.00, 148.77, 141.76, 140.47, 140.04, 139.27, 138.80, 137.50, 137.11, 131.27, 130.67, 129.15, 129.07, 126.98, 123.62, 120.84, 26.19$  (CH<sub>3</sub>); ES MS ( $\text{CH}_3\text{NO}_2$ ):  $m/z$  (relative intensity, %): 1907 (2)  $[[\text{Cu}_6(\mathbf{7d})_3(\mathbf{8})_2](\text{PF}_6)_4]^{2+}$ , 1223.4 (25)  $[[\text{Cu}_6(\mathbf{7d})_3(\mathbf{8})_2](\text{PF}_6)_3]^{3+}$ , 881.2 (49)  $[[\text{Cu}_6(\mathbf{7d})_3(\mathbf{8})_2](\text{PF}_6)_2]^{4+}$ , 675.9 (100)  $[[\text{Cu}_6(\mathbf{7d})_3(\mathbf{8})_2](\text{PF}_6)]^{5+}$ ; UV/Vis ( $\text{CH}_2\text{Cl}_2$ ):  $\lambda$  [nm]

( $\epsilon$  [ $\text{mol}^{-1}\text{dm}^3\text{cm}^{-1}$ ]): 260 (168439), 347 (294489), 388 sh (144446), 560 (33651), 680 (15814); elemental analysis calcd. for  $\text{C}_{198}\text{H}_{138}\text{Cu}_6\text{F}_{36}\text{N}_{24}\text{P}_6$  (%): C 57.94, H 3.39, N 8.19; found C 58.19, H 3.18, N 8.25.

**5:** From **7e** (0.025 g,  $5.40 \times 10^{-5}$  mol), **8** (0.025 g,  $3.62 \times 10^{-5}$  mol) and  $[\text{Cu}(\text{CH}_3\text{CN})_4](\text{PF}_6)_2$  (0.040 g,  $1.07 \times 10^{-4}$  mol) was obtained a solid which was purified by flash chromatography eluting with 4% MeOH/ $\text{CH}_2\text{Cl}_2$  and recrystallisation from MeNO<sub>2</sub>/toluene to yield **5** (0.042 g, 58%) as permanganate-coloured crystals. <sup>1</sup>H NMR ( $\text{CD}_3\text{NO}_2$ , 500 MHz, 25 °C):  $\delta = 8.43$  (d,  $J_{6,4} = 1.9$  Hz, 6H; **7eH-6'**), 8.17 (d,  $J_{3,4} = 8.7$  Hz, 6H; **7eH-3'**), 8.11 (d,  $J_{3,4} = 8.1$  Hz, 6H; **7eH-3**), 8.07 (dd,  $J_{4,3} = 8.5$  Hz,  $J_{4,6} = 2.0$  Hz, 6H; **7eH-4'**), 7.95 (t,  $J_{4,3,4,5} = 7.9$  Hz, 6H; **7eH-4**), 7.54 (s, 12H; **7e** central phenyl H-2'', 3'', 5'', 6''), 7.49 (d,  $J_{\text{om}} = 8.2$  Hz, 24H; **8H-ortho**), 7.31 (d,  $J_{5,4} = 7.7$  Hz, 6H; **7eH-5**), 6.98 (t,  $J_{\text{pm}} = 7.6$  Hz, 12H; **8H-para**), 6.81 (t,  $J_{\text{m,om,p}} = 7.9$  Hz, 24H; **8H-meta**), 2.24 (s, 18H; **7e-CH<sub>3</sub>**); <sup>13</sup>C NMR ( $\text{CD}_3\text{NO}_2$ , 75 MHz, 25 °C):  $\delta = 159.11, 157.96, 152.43, 152.19, 151.67, 141.87, 140.51, 140.17, 138.81, 133.33, 131.32, 130.64, 129.12, 127.44, 124.10, 123.19, 123.14, 121.23, 95.14$  (C≡C), 88.13 (C≡C); ES MS ( $\text{CH}_3\text{NO}_2$ ):  $m/z$  (relative intensity; %): 1865 (3)  $[[\text{Cu}_6(\mathbf{7e})_3(\mathbf{8})_2](\text{PF}_6)_4]^{2+}$ , 1195.4 (33)  $[[\text{Cu}_6(\mathbf{7e})_3(\mathbf{8})_2](\text{PF}_6)_3]^{3+}$ , 860.1 (69)  $[[\text{Cu}_6(\mathbf{7e})_3(\mathbf{8})_2](\text{PF}_6)_2]^{4+}$ , 659.0 (100)  $[[\text{Cu}_6(\mathbf{7e})_3(\mathbf{8})_2](\text{PF}_6)]^{5+}$ ; UV/Vis ( $\text{CH}_2\text{Cl}_2$ ):  $\lambda$  [nm] ( $\epsilon$  [ $\text{mol}^{-1}\text{dm}^3\text{cm}^{-1}$ ]): 362 (325097), 374 (314365), 559 (31038), 677 (13843); IR ( $\text{cm}^{-1}$ ):  $\tilde{\nu} = 3104$  sh, 3085 sh, 3058 m, 3028 sh, 2200 sh, 2220 (C≡C), 1624 w, 1603 m, 1576 w, 1559 m, 1507 m, 1458 s, 1406 w, 1370 s, 1320 w, 1293 w, 1272 m, 1251 m, 1235 m, 1207 m, 1181 m, 1148 m, 1103 w, 1076 w, 1030 m, 1017 m, 1000 m, 937 w, 920 w, 843 s, 801 s, 773 m, 761 m, 752 m, 722 m, 701 s, 644 w, 623 w, 610 m, 598 sh, 557 s, 406 w; elemental analysis calcd. for  $\text{C}_{192}\text{H}_{126}\text{Cu}_6\text{F}_{36}\text{N}_{24}\text{P}_6$  (%): C 57.36, H 3.16, N 8.36; found C 57.16, H 3.28, N 8.48.

**6:** From **7f** (0.030 g,  $5.57 \times 10^{-5}$  mol), **8** (0.026 g,  $3.76 \times 10^{-5}$  mol) and  $[\text{Cu}(\text{CH}_3\text{CN})_4](\text{PF}_6)_2$  (0.042 g,  $1.13 \times 10^{-4}$  mol) was obtained a solid which was purified by flash chromatography eluting first with 4% MeOH/ $\text{CH}_2\text{Cl}_2$  then 8% MeOH/ $\text{CH}_2\text{Cl}_2$ . The chromatography was repeated with 2% MeOH/ $\text{CH}_2\text{Cl}_2$  and the product recrystallised from MeNO<sub>2</sub>/benzene to yield **6** (0.044 g, 56%) as permanganate-coloured microcrystals. <sup>1</sup>H NMR ( $\text{CD}_3\text{NO}_2$ , 500 MHz, 25 °C):  $\delta = 8.51$  (d,  $J_{6,4} = 1.3$  Hz, 6H; **7fH-6'**), 8.19 (d,  $J_{3,4} = 8.6$  Hz, 6H; **7fH-3'**), 8.12 (d,  $J_{3,4} = 8.1$  Hz, 6H; **7fH-3**), 8.08 (dd,  $J_{4,3} = 8.5$  Hz,  $J_{4,6} = 2.0$  Hz, 6H; **7fH-4'**), 7.98 (t,  $J_{4,3,4,5} = 7.9$  Hz, 6H; **7fH-4**), 7.61 (d,  $J_{3',2',5',6'} = 8.5$  Hz, 12H; **7f** biphenyl outer H-3'', 5''), 7.50 (d,  $J_{\text{om}} = 8.2$  Hz, 24H; **8H-ortho**), 7.42 (d,  $J_{2',3',6',5'} = 8.5$  Hz, 12H; **7f** biphenyl inner H-2'', 6''), 7.37 (d,  $J_{5,4} = 7.8$  Hz, 6H; **7fH-5**), 7.00 (t,  $J_{\text{pm}} = 7.5$  Hz, 12H; **8H-para**), 6.82 (t,  $J_{\text{m,om,p}} = 7.9$  Hz, 24H; **8H-meta**), 2.29 (s, 18H; **7f-CH<sub>3</sub>**); <sup>13</sup>C NMR ( $\text{CD}_3\text{NO}_2$ , 125.8 MHz, 25 °C):  $\delta = 159.01, 157.79, 152.55, 151.86, 151.63, 142.03, 141.55, 140.78, 140.22, 138.89, 133.65, 131.26, 130.58, 129.10, 128.51, 127.42, 123.56, 123.03, 122.80, 121.12, 95.65$  (C≡C), 87.04 (C≡C), 26.40 (CH<sub>3</sub>); ES MS ( $\text{CH}_3\text{NO}_2$ ):  $m/z$  (relative intensity; %): 1979 (2)  $[[\text{Cu}_6(\mathbf{7f})_3(\mathbf{8})_2](\text{PF}_6)_4]^{2+}$ , 1271.6 (40)  $[[\text{Cu}_6(\mathbf{7f})_3(\mathbf{8})_2](\text{PF}_6)_3]^{3+}$ , 917.2 (79)  $[[\text{Cu}_6(\mathbf{7f})_3(\mathbf{8})_2](\text{PF}_6)_2]^{4+}$ , 704.6 (100)  $[[\text{Cu}_6(\mathbf{7f})_3(\mathbf{8})_2](\text{PF}_6)]^{5+}$ , 563.0 (16)  $[[\text{Cu}_6(\mathbf{7f})_3(\mathbf{8})_2]^{6+}$ ; UV/Vis ( $\text{CH}_2\text{Cl}_2$ ):  $\lambda$  [nm] ( $\epsilon$  [ $\text{mol}^{-1}\text{dm}^3\text{cm}^{-1}$ ]): 280 (136976), 375 (358542), 571 (25483), 678 (11208); IR ( $\text{cm}^{-1}$ ):  $\tilde{\nu} = 3059$  w, 3034 w, 2217 m (C≡C), 1603 m, 1559 m, 1498 s, 1459 s, 1370 s, 1294 w, 1274 w, 1251 m, 1235 m, 1209 m, 1181 m, 1154 m, 1104 w, 1075 w, 1030 m, 1017 m, 1004 m, 843 s, 801 s, 772 m, 761 m, 752 m, 739 w, 722 m, 701 s, 622 w, 610 m, 597 sh, 558 s, 406 w.

**Crystallographic measurements: 1d:** Single crystals suitable for X-ray crystallography were grown by slow diffusion of benzene into a nitromethane solution of the complex at ambient temperature. X-ray data:  $\text{C}_{162}\text{H}_{114}\text{Ag}_6\text{N}_{24} \cdot 6\text{CF}_3\text{SO}_3 \cdot 7\text{C}_6\text{H}_6$ ,  $M = 4172.7$ ,  $a = 29.099(9)$ ,  $b = 16.618(12)$ ,  $c = 41.128(20)$  Å,  $\beta = 100.92(2)^\circ$ ,  $V = 19528(18)$  Å<sup>3</sup>,  $T = 200$  K, space group =  $C2/c$ ,  $Z = 4$ ,  $\rho_{\text{calcd}} = 1.42$  g cm<sup>-3</sup>,  $\mu(\text{MoK}\alpha) = 0.74$  mm<sup>-1</sup>,  $F(000) = 8400$ . Data were collected on a STOE-IPDS diffractometer,  $7.4^\circ > 2\theta > 48.3^\circ$ , MoK $\alpha$  radiation (graphite monochromator). A total of 14434 independent reflections were measured and of these, 11217 had  $|F_0| \geq 4\sigma(F_0)$  and were considered to be observed. The data were corrected for Lorentz and polarisation factors; no absorption correction was applied. The structure was solved by direct methods. The Hydrogen atoms were placed in calculated positions, the isotropic temperature factor was coupled with the  $U_{\text{eq}}$  from the parent carbon atom. The refinement was by full-matrix least-squares based on  $F^2$  to give  $R = 0.0831$ ,  $wR = 0.2068$  with  $F > 6\sigma(F_0)$ .  $R = 0.1078$ ,  $wR = 0.2406$  with all data for 1108 parameters. The maximum and minimum residual electron densities in the final  $\Delta F$  map were 1.566 and  $-1.278$  e Å<sup>-3</sup>. **10:** Single crystals suitable for X-ray

crystallography were grown by slow diffusion of benzene into a nitromethane solution of the complex at ambient temperature. X-ray data:  $C_{168}H_{126}Cu_6N_{24} \cdot 6PF_6 \cdot 6.5C_6H_6 \cdot 4.5CH_3NO_2$ ,  $M = 4514.5$ , monoclinic,  $a = 26.843(3)$ ,  $b = 39.511(3)$ ,  $c = 19.505(2)$  Å,  $\beta = 91.92(1)^\circ$ ,  $V = 20675(4)$  Å<sup>3</sup>,  $T = 200$  K, space group =  $P2(1)/n$ ,  $Z = 4$ ,  $\rho_{\text{calcd}} = 1.45$  g cm<sup>-3</sup>,  $\mu(\text{MoK}\alpha) = 0.75$  mm<sup>-1</sup>,  $F(000) = 9228$ . Data were collected on a STOE-IPDS diffractometer,  $3.1^\circ > 2\theta < 50.2^\circ$ ,  $\text{MoK}\alpha$  radiation (graphite monochromator). A total of 34653 independent reflections were measured and of these, 25538 had  $|F_0| > 4\sigma(|F_0|)$  and were considered to be observed. The data were corrected for Lorentz and polarisation factors; no absorption correction was applied. The structure was solved by direct methods. The Hydrogen atoms were placed in calculated positions, the isotropic temperature factor was coupled with the Ueq from the parent carbon atom. The refinement was by full-matrix least-squares based on  $F^2$  to give  $R = 0.0629$ ,  $wR = 0.1731$  with  $F > 4\sigma(F_0)$ .  $R = 0.0850$ ,  $wR = 0.1905$  with all data for 2663 parameters. The maximum and minimum residual electron densities in the final  $\Delta F$  map were 0.906 and  $-0.642$  e Å<sup>-3</sup>. Further details of the crystal structure investigations can be obtained from the Fachinformationszentrum Karlsruhe, D-76344 Eggenstein-Leopoldshafen, Germany (fax: (+49) 7247-808-666; e-mail: crysdata@fiz-karlsruhe.de), on quoting the depository numbers CSD-410250 (**1d**) and CSD-410251 (**10**).

## Acknowledgements

We would like to thank the Collège de France for financial support (P.N.W.B.), Dr A. Dupont-Gervais, Dr. E. Leize and Dr. A. Van Dorsseleer for the ES MS and Dr. R. Graff for the COSY and NOESY measurements.

- [1] B. Dietrich, P. Viout, J.-M. Lehn, *Macrocyclic Chemistry; Aspects of Organic and Inorganic Supramolecular Chemistry*, VCH, Weinheim, Germany, **1993**, chapter 3, p. 241.
- [2] For reviews on the synthesis of cyclophanes, see: *Comprehensive Supramolecular Chemistry*, Vol. 2 (Eds. J. L. Atwood, J. E. D. Davies, D. D. MacNicol, F. Vögtle, J.-M. Lehn), Pergamon, Oxford, **1996**.
- [3] a) D. J. Cram, J. M. Cram, *Container Molecules and Their Guests; Monographs in supramolecular chemistry* (Ed.: J. F. Stoddart), Royal Society of Chemistry, **1994**. Chapter 7, p. 131; b) E. Maverick, D. J. Cram, reference [2], chapter 12, p. 367.
- [4] A. Müller, H. Reuter, S. Dillinger, *Angew. Chem.* **1995**, *107*, 2505–2539; *Angew. Chem. Int. Ed. Engl.* **1995**, *34*, 2328.
- [5] a) J.-M. Lehn, *Supramolecular Chemistry: Concepts and Perspectives*, VCH, Weinheim, **1995**, chapter 9, p. 139; b) D. Philp, J. F. Stoddart, *Angew. Chem.* **1996**, *108*, 1242; *Angew. Chem. Int. Ed. Engl.* **1996**, *35*, 1154.
- [6] a) J. Rebek Jr., *Chem. Soc. Rev.* **1996**, 255; b) J. Rebek Jr, *Pure Appl. Chem.* **1996**, *68*, 1261; c) M. M. Conn, J. Rebek Jr, *Chem. Rev.* **1997**, *97*, 1647.
- [7] P. N. W. Baxter, J.-M. Lehn, A. DeCian, J. Fischer, *Angew. Chem.* **1993**, *105*, 92; *Angew. Chem. Int. Ed. Engl.* **1993**, *32*, 69.
- [8] a) F. G. M. Niele, R. J. M. Nolte, *J. Am. Chem. Soc.* **1988**, *110*, 172; b) R. W. Saalfrank, A. Stark, K. Peters, H.-G. von Schnering, *Angew. Chem.* **1988**, *100*, 878; *Angew. Chem. Int. Ed. Engl.* **1988**, *27*, 851; c) R. W. Saalfrank, A. Stark, M. Bremer, H.-U. Hummel, *Angew. Chem.* **1990**, *102*, 292; *Angew. Chem. Int. Ed. Engl.* **1990**, *29*, 311; d) J.-F. You, G. C. Papaefthymiou, R. H. Holm, *J. Am. Chem. Soc.* **1992**, *114*, 2697; e) R. W. Saalfrank, B. Hörner, D. Stalke, J. Salbeck, *Angew. Chem.* **1993**, *105*, 1223; *Angew. Chem. Int. Ed. Engl.* **1993**, *32*, 1179; f) R. W. Saalfrank, R. Burak, A. Breit, D. Stalke, R. Herbst-Irmer, J. Daub, M. Porsch, E. Bill, M. Mütther, A. X. Trautwein, *Angew. Chem.* **1994**, *106*, 1697; *Angew. Chem. Int. Ed. Engl.* **1994**, *33*, 1621; g) K. Fujimoto, S. Shinkai, *Tetrahedron Lett.* **1994**, *35*, 2915; h) R. W. Saalfrank, R. Burak, S. Reihls, N. Löw, F. Hampel, H.-D. Stachel, J. Lentmaier, K. Peters, E.-M. Peters, H.-G. von Schnering, *Angew. Chem.* **1995**, *107*, 1085; *Angew. Chem. Int. Ed. Engl.* **1995**, *34*, 993; i) M. Fujita, S. Nagao, K. Ogura, *J. Am. Chem. Soc.* **1995**, *117*, 1649; j) M. Fujita, D. Oguro, M. Miyazawa, H. Oka, K. Yamaguchi, K. Ogura, *Nature*, **1995**, *378*, 469; k) T. Beissel, R. E. Powers, K. N. Raymond, *Angew. Chem.* **1996**, *108*, 1166; *Angew. Chem. Int. Ed. Engl.* **1996**, *35*, 1084; l) S. Mann, G. Huttner, L. Zsolnai, K. Heinze, *Angew. Chem.* **1996**, *108*, 2983; *Angew. Chem. Int. Ed. Engl.* **1996**, *35*, 2808; m) P. Jacopozzi, E. Dalcanale, *Angew. Chem.* **1997**, *109*, 665; *Angew. Chem. Int. Ed. Engl.* **1997**, *36*, 613; n) C. M. Hartshorn, P. J. Steel, *J. Chem. Soc. Chem. Commun.* **1997**, 541; o) P. J. Stang, B. Olenyuk, D. C. Muddiman, R. D. Smith, *Organometallics*, **1997**, *16*, 3094; p) for earlier examples of metal-ion-assembled cage complexes, see: P. N. W. Baxter in *Comprehensive Supramolecular Chemistry*, Vol. 9 (Eds. J. L. Atwood, J. E. D. Davies, D. D. MacNicol, F. Vögtle, J.-M. Lehn), Pergamon, Oxford, **1996**, p. 165.
- [9] For discussions concerning bacterial cell surface (S-layer) assemblies, see: a) U. B. Sleytr, M. Sára, *Tibtech.* **1997**, *15*, 20, and references therein; for virus capsid assembly see: b) A. Klug, *Angew. Chem.* **1983**, *95*, 579; *Angew. Chem. Int. Ed. Engl.* **1983**, *22*, 565.
- [10] a) ref. [5a] p. 144; b) E. C. Constable, in reference [8p], vol. 9, p. 213.
- [11] C. Piguet, *Chem. Rev.* **1997**, *97*, 2005.
- [12] J.-C. Chambron, C. Dietrich-Buchecker, J. P. Sauvage, in reference [8p], vol. 9, p. 43.
- [13] A. W. Maverick, M. L. Ivie, J. H. Waggenspack, F. R. Fronczek, *Inorg. Chem.* **1990**, *29*, 2403.
- [14] Initial ESMS studies into the reaction between **8** and varying ratios of  $[\text{Cu}(\text{CH}_3\text{CN})_4](\text{PF}_6)$  showed that the dominant reaction products were  $[\text{Cu}(\mathbf{8})]^+$  and  $[\text{Cu}(\mathbf{8})_2]^+$  along with smaller, varying amounts of  $[\text{Cu}_2(\mathbf{8})_3]^+$  at  $10^{-5}$ – $10^{-3}$  mol dm<sup>-3</sup> in MeNO<sub>2</sub> and MeCN/CH<sub>2</sub>Cl<sub>2</sub> mixtures. The precipitation of insoluble polymers occurred only at higher concentrations and upon standing for several days. Also, combination of **8**, 6,6'-dimethyl-2,2'-bipyridine (6,6'-Me<sub>2</sub>-bipy) and  $[\text{Cu}(\text{CH}_3\text{CN})_4](\text{PF}_6)$  in a 1:3:3 stoichiometric ratio in MeCN/CH<sub>2</sub>Cl<sub>2</sub> or MeNO<sub>2</sub> yielded an equilibrium mixture of 80–90%  $[\text{Cu}_3(\mathbf{8})(6,6'\text{-Me}_2\text{-bipy})_3](\text{PF}_6)_3$  and species resulting from the partial dissociation of this complex. This evidence suggested that ligand **8** would be a viable candidate for the successful generation of the cage **1**.
- [15] B. Kohne, K. Praefcke, *Liebigs Ann. Chem.* **1985**, 522.
- [16] CAChe (Oxford Molecular Group Inc. 1995)
- [17] J.-M. Lehn, R. Ziessel, *Helv. Chim. Acta*, **1988**, *71*, 1511.
- [18] For the isolation of a single supramolecular species through crystallisation from an equilibrium mixture of circular inorganic Cu<sup>I</sup>-containing architectures (i. e. from an inorganic virtual combinatorial library) see: P. N. W. Baxter, J.-M. Lehn, K. Rissanen, *J. Chem. Soc. Chem. Commun.* **1997**, 1323.
- [19] a) R. Krämer, J. M.-Lehn, A. Marquis-Rigault, *Proc. Natl. Acad. Sci. USA*, **1993**, *90*, 5394; b) D. P. Funeriu, Y.-B. He, H.-J. Bister, J.-M. Lehn, *Bull. Soc. Chim. Fr.* **1996**, *133*, 673.
- [20] Other structural motifs designed and generated via mixed ligand multicomponent metal-ion-mediated self-assembly include ladder architectures: a) P. N. W. Baxter, G. S. Hanan, J.-M. Lehn, *J. Chem. Soc. Chem. Commun.* **1996**, 2019; a [2 × 3]G rectangular grid; b) P. N. W. Baxter, J.-M. Lehn, B. O. Kneisel, D. Fenske, *Angew. Chem.* **1997**, *109*, 2067; *Angew. Chem. Int. Ed. Engl.* **1997**, *36*, 1978; a heteroduplex helicate; c) B. Hasenknopf, J.-M. Lehn, G. Baum, D. Fenske, *Proc. Natl. Acad. Sci. USA*, **1996**, *93*, 1397; pseudorotaxane racks: d) H. Sleiman, P. N. W. Baxter, J.-M. Lehn, K. Rissanen, *J. Chem. Soc. Chem. Commun.* **1995**, 715; e) P. N. W. Baxter, H. Sleiman, J.-M. Lehn, K. Rissanen, *Angew. Chem.* **1997**, *109*, 1350; *Angew. Chem. Int. Ed. Engl.* **1997**, *36*, 1294; f) H. Sleiman, P. N. W. Baxter, J.-M. Lehn, K. Rissanen, K. Aerola, *Inorg. Chem.* **1997**, *36*, 4734; pseudorotaxanes: g) J.-C. Chambron, C. O. Dietrich-Buchecker, J.-F. Nierengarten, J.-P. Sauvage, *J. Chem. Soc. Chem. Commun.* **1993**, 801; h) J.-P. Collin, P. Gaviña, J.-P. Sauvage, *J. Chem. Soc. Chem. Commun.* **1996**, 2005; and rotaxanes: i) J.-C. Chambron, C. O. Dietrich-Buchecker, V. Heitz, J.-P. Sauvage, *J. Chem. Soc. Chem. Commun.* **1992**, 1131; j) D. J. Cárdenas, P. Gaviña, J.-P. Sauvage, *J. Chem. Soc. Chem. Commun.* **1996**, 1915; k) N. Solladié, J.-C. Chambron, C. O. Dietrich-Buchecker, J.-P. Sauvage, *Angew. Chem.* **1996**, *108*, 957; *Angew. Chem. Int. Ed. Engl.* **1996**, *35*, 906.
- [21] Helicates have however been found to form upon reaction between oligobipyridine ligands and CuCl in water, A. Marquis-Rigault, J. M. Lehn, unpublished results.
- [22] a) M. Munakata, S. Kitagawa, A. Asahara, H. Masuda, *Bull. Chem. Soc. Jpn.* **1987**, *60*, 1927–1929; b) J. F. Dobson, B. E. Green, P. C. Healy, C. H. L. Kennard, C. Pakawatchai, A. H. White, *Aust. J. Chem.*

- 1984**, 37, 649; c) P. J. Burke, D. R. McMillin, W. R. Robinson, *Inorg. Chem.* **1980**, 19, 1211.
- [23] The distortions from ideal tetrahedral coordination geometry in  $[M(L)]^+$  ( $M = Cu^+$ ,  $Ag^+$ ;  $L =$  bipyridine and phenanthroline ligands) complexes is currently accepted to originate principally from the maximisation of intercation ligand  $\pi$ - $\pi$  interactions rather than Jahn–Teller effects. For a discussion of this matter, see: K. V. Goodwin, D. R. McMillin, W. R. Robinson, *Inorg. Chem.* **1986**, 25, 2033.
- [24] A detailed study of the anion inclusion properties of **1** will be reported elsewhere: P. N. W. Baxter, J.-M. Lehn, unpublished results.
- [25] This approach has recently been used in the  $Cu^I$ -mediated assembly of macrocyclic structures, M. Schmittel, A. Ganz, *J. Chem. Soc. Chem. Commun.* **1997**, 999.
- [26] Synthesis of the above and related ligand structures will be reported elsewhere.
- [27] P. N. W. Baxter, J.-M. Lehn, G. Baum, B. Kneisel, D. Fenske, *Chem. Eur. J.* **1999**, 5, 113.

Received: August 17, 1998 [F 1309]